Mammalian-specific ectodermal enhancers control the expression of *Hoxc* genes in developing nails and hair follicles

Marc Fernandez-Guerrero[a], Nayuta Yakushiji-Kaminatsui[b,1], Lucille Lopez-Delisle[b], Sofía Zdral[a], Fabrice Darbellay[b,2], Rocío Perez-Gomez[a], Christopher Chase Bolt[b], Manuel A. Sanchez-Martin[c], Denis Duboule[b,d,e,3], and Marian A. Ros[a,f,3]

[a]Instituto de Biomedicina y Biotecnología de Cantabria, Consejo Superior de Investigaciones Científicas–Universidad de Cantabria–Sociedad para el Desarrollo de Cantabria, 39011 Santander, Spain; [b]School of Life Sciences, Federal Institute of Technology, Lausanne, 1015 Lausanne, Switzerland; [c]Department of Medicine, University of Salamanca, 37007 Salamanca, Spain; [d]Department of Genetics and Evolution, University of Geneva, 1211 Geneva 4, Switzerland; [e]Collège de France, Paris, France; and [f]Departamento de Anatomía y Biología Celular, Facultad de Medicina, Universidad de Cantabria, 39011 Santander, Spain

Contributed by Denis Duboule, October 6, 2020 (sent for review June 1, 2020; reviewed by Nadav Ahituv and Robert Hill)

Vertebrate *Hox* genes are critical for the establishment of structures during the development of the main body axis. Subsequently, they play important roles either in organizing secondary axial structures such as the appendages, or during homeostasis in postnatal stages and adulthood. Here, we set up to analyze their elusive function in the ectodermal compartment, using the mouse limb bud as a model. We report that the *HoxC* gene cluster was co-opted to be transcribed in the distal limb ectoderm, where it is activated following the rule of temporal colinearity. These ectodermal cells subsequently produce various keratinized organs such as nails or claws. Accordingly, deletion of the *HoxC* cluster led to mice lacking nails (anonychia), a condition stronger than the previously reported loss of function of *Hoxc13*, which is the causative gene of the ectodermal dysplasia 9 (ECTD9) in human patients. We further identified two mammalian-specific ectodermal enhancers located upstream of the *HoxC* gene cluster, which together regulate *Hoxc* gene expression in the hair and nail ectodermal organs. Deletion of these regulatory elements alone or in combination revealed a strong quantitative component in the regulation of *Hoxc* genes in the ectoderm, suggesting that these two enhancers may have evolved along with the mammalian taxon to provide the level of HOXC proteins necessary for the full development of hair and nail.

Hox genes | enhancers | nails | hair follicles | transcription

In most bilateria, genes members of the *Hox* family of transcription factors are important for the proper organization of structures along the main body axis, during early development. On top of this major task, vertebrate *Hox* genes are also necessary for the morphogenesis of a variety of secondary structures such as the appendages or the external genitalia (1). In amniotes, *Hox* genes are organized in four clusters (*HoxA*, *B*, *C*, and *D*), all of them being involved in the development of the trunk axis. Subsequently however, subgroups of gene clusters display some specificities for particular tissues or structures. For example, both the *HoxA* and *HoxD* clusters are essential for the organization of the tetrapod limb morphology (2–7), while the deletion of both *HoxA* and *HoxB* clusters leads to severe cardiac malformations, not detected in any of the single deletion mutants. Likewise, deletions of both the *HoxA* and *HoxC* clusters induced a complete renal aplasia, which was not detected with either deletion alone (8).

Such a functional redundancy between *Hox* clusters can be explained by their patterns of duplication during the evolution of vertebrates, with particular functional traits being conserved in all or some gene clusters after duplication (8). In this context, *Hox* gene function associated with recent vertebrate features, i.e., features that must have appeared late, after the two rounds of duplication, can be expected to involve single gene clusters and thus to show less functional redundancy. Examples of this situation may be found either in the function of some *Hoxa* genes in uterine physiology (9–11) or in the apparent specialization of some *Hoxc* genes for epidermal derivatives (12, 13), while other clusters apparently do not play any detectable function there.

Indeed, while the single deletion of the *HoxC* gene cluster did not reveal any gross phenotype (14), several studies have suggested that *Hoxc* genes are involved in the development of ectodermal organs (12, 15). The fact that such organs usually become fully developed after birth explains why the full *HoxC* cluster deletion, which is lethal at birth because of respiratory problems (14), did not unmask these functional contributions. However, both expression and inactivation studies have revealed potential contributions, in particular at late fetal stages as well as during postnatal development and even adulthood (12, 16, 17).

Significance

In this study, we report a unique and necessary function for the *HoxC* gene cluster in the development of some ectodermal organs, as illustrated both by the hair and nail phenotype displayed by mice lacking the *Hoxc13* function and by the congenital anonychia (absence of nails) in full *HoxC* cluster mutants. We show that *Hoxc* genes are activated in a colinear manner in the embryonic limb ectoderm and are subsequently transcribed in developing nails and hairs. We identify two mammalian-specific enhancers located upstream of the *HoxC* cluster, which display an exclusive ectodermal specificity. Individual or combined enhancer deletions suggest that they act in combination to raise the transcription level of several *Hoxc* genes during hair and nail development.

Author contributions: N.Y.-K., D.D., and M.A.R. designed research; M.F.-G., N.Y.-K., S.Z., F.D., R.P.-G., M.A.S.-M., D.D., and M.A.R. performed research; C.C.B. contributed new reagents/analytic tools; M.F.-G., N.Y.-K., L.L.-D., D.D., and M.A.R. analyzed data; and L.L.-D., D.D., and M.A.R. wrote the paper.

Reviewers: N.A., University of California San Francisco Medical Center; and R.H., The University of Edinburgh.

The authors declare no competing interest.

[1]Present address: Laboratory for Developmental Genetics, RIKEN Center for Integrative Medical Sciences, Yokohama, Kanagawa 230-0045, Japan.

[2]Present address: Environmental Genomics and Systems Biology Division, Lawrence Berkeley Laboratories, Berkeley, CA 94720.

[3]To whom correspondence may be addressed. Email: denis.duboule@unige.ch or rosm@unican.es.

This article contains supporting information online at https://www.pnas.org/lookup/suppl/doi:10.1073/pnas.2011078117/-/DCSupplemental.

First published November 16, 2020.

In such instances, some *Hoxc* genes display complex patterns of expression in relation to the differentiation of epidermal organs such as the hairs and nails (12, 15, 18, 19), two ectodermal derivatives that form through epithelial–mesenchymal interactions between the surface ectoderm and the underlying mesoderm, the latter being responsible for the development of site-specific skin derivatives (17, 20).

The morphogenesis of both hairs and nails begins with the induction of ectodermal thickenings or placodes by a subjacent dermal condensate (21). Once the placode forms, signaling events between the ectodermal and mesodermal components drive proliferation of the ectoderm to produce the hair peg or the nail matrix and eventually lead to a mature hair follicle (HF) or nail organ. Both the morphogenetic steps and the signaling molecules involved are remarkably similar during the development of these two integumentary structures (reviewed in refs. 22 and 23), and there is evidence suggesting that *Hoxc* genes may participate in these processes. This is mostly supported by the inactivation of *Hoxc13*, which induced specific hair and nail defects in adult homozygous mutant animals (12, 13). These mice showed long and fragile nails; they lacked vibrissae at birth and subsequently displayed a nude appearance with no external pelage. Although the morphogenesis of HFs appeared normal, hair differentiation was defective with very fragile shafts that broke as soon as they emerged through the skin surface, leading to alopecia. Both the hair and claw defects were associated with defective keratin gene expression, as *Hoxc13* was reported to be an important regulator of various keratin genes (15).

In order to evaluate the regulatory mechanism at work at the *HoxC* locus, i.e., to assay first how many *Hoxc* genes are involved into the development of such epidermal organs and, second, whether a single epidermal regulatory module may control their expression there in a coordinated manner, we selected the developing mouse limb bud as model system, for it allows to microdissect out the ectodermal component from where nails and hairs subsequently arise. We used RNA-seq on this isolated ectodermal jacket during both the early patterning phase and also the subsequent phase of tissue-specific differentiation. Here, we show that *Hoxc* genes, unlike both *Hoxa* and *Hoxd* genes, are specifically expressed in a colinear manner in the limb bud ectoderm. At later fetal stages, expression becomes localized in the developing nail region and HFs. Accordingly, we report that mice lacking the *HoxC* cluster suffer from anonychia (absence of nail or claw) at birth. We show that this global transcriptional control is largely associated with two *cis*-regulatory regions and that only the deletion of both enhancers together led to a phenotype involving a disheveled fur and hypoplastic nails. Finally, the removal of both enhancers in a weakened *HoxC* genetic background caused a striking cyclic alopecia. We conclude that the *HoxC* cluster was evolutionary co-opted for exerting an essential function during the development of mammalian the integuments. As reported for other *Hox* clusters in different contexts, this co-option was at least partly achieved through the emergence of remote enhancers with ectodermal specificities.

Results

Colinear Expression of *Hoxc* Genes in the Limb Bud Ectoderm. Initially, we set out to study in detail how *Hoxc* genes are regulated in the developing limb by carefully isolating the ectodermal layer from the mesoderm component. To this aim, we generated RNA-seq datasets of both microdissected mouse distal forelimb mesenchymal progenitors and the overlying ectodermal cells at four consecutive developmental stages. We selected embryonic day 9.5 (E9.5), E10.5, E11.5, and E12.5 limb buds because they illustrate a wide range of processes, from the early emergence of the limb bud to the specification of the digits. Due to the progressive proximo-distal development of the limb bud, our analysis was restricted to the distal 150 μm, which is considered a good approximation of the progress zone (24–26). As a consequence, we microdissected a 150-μm-thick band of the distal limb bud, and the mesoderm and ectoderm components were separated by mild trypsin digestion and processed separately (*SI Appendix*, Fig. S1*A* and *Materials and Methods*). Two biological replicates were collected per stage, and each pair of ectoderm and mesoderm replicates was obtained from the same batch of embryos.

Because a few mesoderm cells could occasionally remain attached to the ectoderm during dissection, potentially contaminating the ectodermal samples, we evaluated the purity of samples by analyzing the expression of genes known to be expressed exclusively in the ectoderm or mesoderm components of limb buds. *Fgf8*, *Sp6*, *Trp63*, *Perp*, *Krt14*, *Sp8*, and *Wnt7a* were selected as ectoderm specific genes, whereas *Prrx1*, *Tbx5*, *Hoxa9*, *Hoxd10*, *Fgf10*, *Pecam1*, and *Cdh5* were selected as mesoderm specific genes (1, 27–31). A heatmap visualization of the transcription profiles of these genes across samples showed that the separation of the ectoderm and the mesoderm was clean, with a negligible level of contamination between both limb components (*SI Appendix*, Fig. S1*B*), except in replicate 1 of the E11.5 ectoderm samples where a slight contamination with mesodermal cells was scored (Fig. 1*A*).

To evaluate the proximity between samples, we performed a principal-component analysis (PCA). When samples were plotted along the first two components and in two dimensions, the first dimension (PC1), accounting for 75% of the variance, strongly separated the samples according to the ectodermal and mesodermal nature of the tissue. The second dimension (PC2), accounting for 12% of the variance, separated the samples according to the developmental stage (*SI Appendix*, Fig. S1*C*). Hierarchical cluster analysis (HCA) of the 16 samples showed a strong clustering of samples by tissue and between consecutive stages (*SI Appendix*, Fig. S1*D*). Both the PCA and the HCA showed a high consistency between replicates.

We then looked at the tissue specific gene expression dynamics of all *Hox* family members and generated a heatmap using their normalized expression values [$\log_2(1 + \text{FPKM})$]. While this plot expectedly highlighted the known temporal colinear activation of *Hoxa* and *Hoxd* genes in the limb mesoderm (Fig. 1*A*), it revealed a previously overlooked distinctive expression of *Hoxc* genes in the limb ectoderm, with a comparable progressive temporal activation, starting with 3′-located genes and with 5′-located *Hoxc12* and *Hoxc13* gene expression being maximum at the last stage examined (E12.5) (Fig. 1*A*). The visual inspection of coverage from RNA-seq across the *HoxC* cluster confirmed a transition from an initial higher expression of *Hoxc5*, *Hoxc6*, and *Hoxc8* (E9.5 and E10.5) to a higher expression of *Hoxc12* and *Hoxc13* at later stages (E11.5 and E12.5) (Fig. 1*B*). Genes with an intermediate position in the cluster such as *Hoxc9*, *Hoxc10*, and *Hoxc11* were also sequentially activated, but their level of expression did not reach that of the genes located at both extremities of the cluster, at least during the period under scrutiny. Therefore, the expression dynamics of *Hoxc* genes in the limb bud ectoderm follows the typical temporal colinear pattern of *Hox* genes expression (32).

In order to validate these results and to determine the spatial distribution of *Hoxc* transcripts in the limb ectoderm, we used in situ hybridization (ISH) on tissue sections, which showed a clear restriction of expression to the ectodermal monolayer (Fig. 1*C*, arrowheads). As the limb bud emerged (E9.5), the expression of 3′-located *Hoxc* genes covered the whole limb bud ectoderm, whereas, at later stages (E12.5), the expression of 5′-located genes appeared more restricted to the tip of the limb bud (Fig. 1*C*). Subsequently, at E14.5, *Hoxc12* and *Hoxc13* transcripts were found concentrated in the digit tips, as detected by ISH both in whole-mount and tissue sections and progressively confined to the developing nail region (E16.5) (Fig. 1 *D* and *E*). In

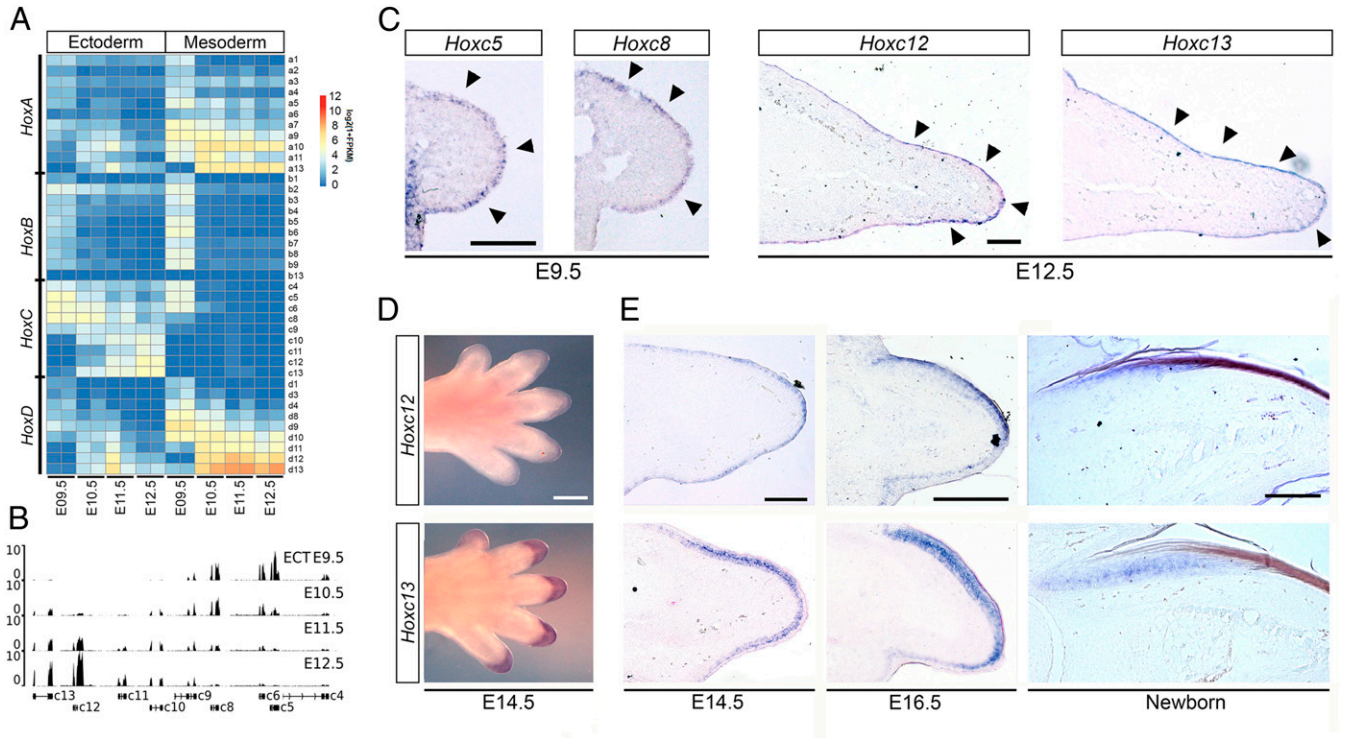

Fig. 1. Colinear activation of *Hoxc* genes in the limb ectoderm. (*A*) Heatmap showing the $\log_2(1 + \text{FPKM})$ values of all *Hox* genes across the samples. *Hoxc* genes are activated in the ectoderm following a temporal sequence. The ectoderm and mesoderm samples were obtained as indicated in *SI Appendix*, Fig. S1*A*. (*B*) Expression profiles of *HoxC* cluster genes in the four ectodermal (ECT) stages analyzed. Data were normalized to the million uniquely mapped reads, and mean of duplicates is presented. (*C*) mRNA ISH in tissue sections showing expression of *Hoxc5* and *Hoxc8* in the early E9.5 limb bud ectoderm and of *Hoxc12* and *Hoxc13* in the late E12.5 limb bud ectoderm. Arrowheads indicate the ectodermal restriction of expression ($n = 2$). (Scale bars: 100 μm.) (*D*) Whole-mount ISH showing restriction of *Hoxc12* and *Hoxc13* expression to the forelimb digit tips at E14.5 ($n = 3$). (Scale bar: 500 μm.) (*E*) *Hoxc12* and *Hoxc13* transcripts become progressive confined to the dorsal ectoderm over the last phalanx (E16.5) and finally to the nail matrix in newborn ($n = 2$). For components of the nail organ, please see Fig. 2*C*. (Scale bars: 200 μm.) In all sections, dorsal is up, and distal to the right.

newborn mice, *Hoxc13* expression persisted in the nail matrix, while only residual *Hoxc12* transcripts remained in this region (Fig. 1*E*).

Function of *Hoxc* Genes in Nail Development. This expression of *Hoxc* genes in the forelimb ectoderm during these developmental stages and the concentration of mRNAs in the nail region suggested a function for these genes in nail morphogenesis. This was previously illustrated both by the misshaped nail phenotype displayed by mice lacking the function of *Hoxc13* (12), and by the involvement of *HOXC13* in the human ectodermal dysplasia 9 (ECTD9) (Online Mendelian Inheritance in Man [OMIM] 614931) (33) characterized by severe nail dystrophy. Consequently, we carefully examined the nail in mice lacking the entire *HoxC* cluster ($HoxC^{-/-}$), even though these mutant mice die at birth, presumably due to respiratory problems (14).

Visual inspection of $HoxC^{-/-}$ newborn limbs revealed a marked flexion of forelimb digits with a strong suspicion of nail agenesis, based on the lack of the typical light reflection caused by the nail plate, a rich keratinized structure (Fig. 2*A*). Interestingly, congenital ventral contractures of the digits have also been reported in patients with microdeletions involving the *HOXC* cluster in heterozygosis (34). The complete absence of nails was confirmed by histological analyses. In addition to the lack of nail plate, there was no evidence of the nail matrix, neither of a nail bed, and the proximal fold was practically nonexistent, merely reduced to a slight groove (Fig. 2 *B* and *C*, scheme). Therefore, in marked contrast to their wild-type littermates, $HoxC^{-/-}$ mutant newborns showed no evidence of nail morphogenesis at the tip of their digits.

To evaluate the level of epithelial differentiation in the mutant nail region, we used a range of anti-keratin (Krt) antibodies, which altogether confirmed the complete absence of the nail organ in $HoxC^{-/-}$ mutant specimens. For instance, we observed that Krt5, a specific marker of the basal layer, and Krt10, a suprabasal epithelial marker, unexpectedly persisted in the epithelium of the mutant nail region, while they were normally down-regulated in control animals (Fig. 2*D*). In addition, the expression of hard keratins specific for hair and nail, as detected by using the AE13 antibody, was not found in the mutant nail region (Fig. 2*D*). We thus concluded that at birth, the epithelium of the digit tip of $HoxC^{-/-}$ mutants displayed a level of differentiation somewhat similar to that of the interfollicular epithelium in control samples, as generally illustrated by the lack of specific nail differentiation (Fig. 2*D*′, scheme). The analysis of mutant hindlimbs uncovered a similar although slightly milder phenotype (*SI Appendix*, Fig. S2). Again, the expression of hard keratins was not detected while Krt10 abnormally persisted in the digit tip epithelium indicating the impairment of nail differentiation, even though Krt5 was reduced in suprabasal layers. The difference between forelimb and hindlimb could possibly reflect the expression of additional *Hox* genes in the hindlimb ectoderm, a possibility that remains to be assayed.

This previously unnoticed congenital anonychia observed in $HoxC^{-/-}$ mutant animals indicates that *HoxC* cluster genes not only participate to shape the nails, as shown by the *Hoxc13* loss-of-function mutation (12), but are also necessary for their

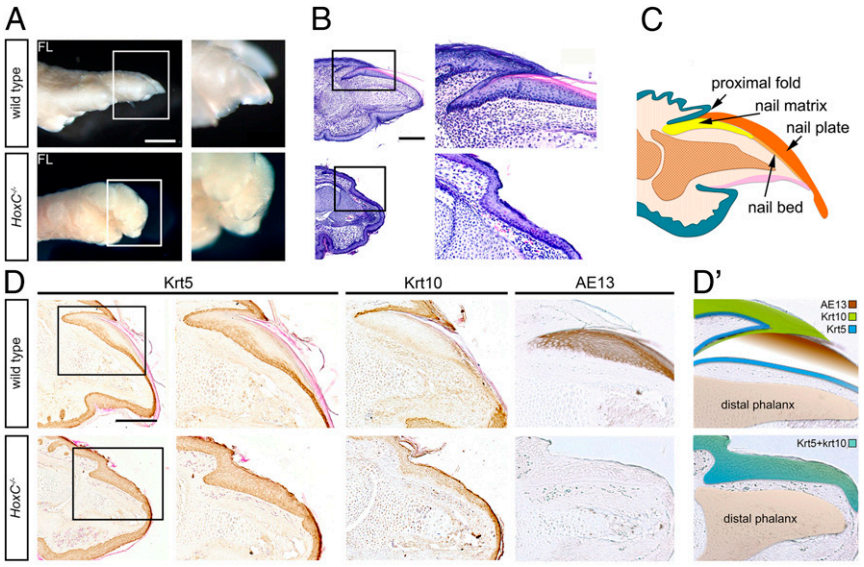

Fig. 2. Congenital anonychia in *HoxC*$^{-/-}$ mutant mice. (*A*) Photographs showing lateral views of the hand of wild-type and *HoxC*$^{-/-}$ newborn mice. Note the pronounced ventral flexion of digits in the mutant specimen. (Scale bar: 1 mm.) (*B*) Hematoxylin-eosin–stained longitudinal section of a forelimb finger, which shows the absence of the nail organ in *HoxC*$^{-/-}$ mutant animals. (Scale bar: 200 μm.) In *A* and *B*, the framed area is magnified on the *Right* (n = 3). (*C*) Schematic representation of the nail organ showing its various components. (*D*) Immunohistochemistry for the detection of Krt5, Krt10, and hard keratins (AE13 antibody) in consecutive longitudinal sections of wild-type and *HoxC*$^{-/-}$ newborn mice. For Krt5 immunostaining, a lower magnification is also shown to frame the area under study (n = 3). (Scale bar: 200 μm.) (*D′*) Schematic representation of the differentiation state of the nail region in *HoxC*$^{-/-}$ mutants. In all sections, dorsal is up, and distal is to the right.

morphogenesis, at least at the proper time. Indeed, we cannot exclude a developmental delay in the differentiation of the nail organ, for the perinatal death of *HoxC*$^{-/-}$ mutant mice precluded further analysis. In *Hoxc13*$^{-/-}$ mice, twisted and fragile nails were reported. At birth, the epithelial differentiation of the nail region, according to Krt5, was similar to normal, but the expression of Krt10 persisted in the suprabasal layers of the nail matrix and hard keratins were not detected (*SI Appendix*, Fig. S3). Therefore, it seems that, in the absence of *Hoxc13* function, other *Hoxc* genes can activate the nail differentiation program, although the expression of the hard keratins specific to the hair and nails appears to depend on *Hoxc13*.

Transcriptional Regulation of *Hoxc* Genes in the Ectoderm. The apparent coordinated function of *Hoxc* genes in limb ectodermal derivatives echoed other well-described cases where several *Hox* genes located *in cis* are controlled by batteries of common long-acting enhancers positioned outside the respective *Hox* cluster (35–37). We investigated this possibility by using ATAC-seq (assay for transposase-accessible chromatin with high-throughput sequencing) to identify accessible chromatin regions in isolated ectodermal hulls of E14.5 digit tips (Fig. 3*A*, first and second tracks). We selected this stage because of the high expression levels of both *Hoxc12* and *Hoxc13*. We used two forelimb replicates and two hindlimb replicates with each dataset individually processed and looked for open chromatin regions within and around the *HoxC* cluster. We identified several open chromatin regions in the *HoxC* cluster itself, which correspond to the activity of *Hoxc* genes, expectedly absent from the control forebrain ATAC-seq dataset. In addition, two focal regions of significant ATAC-seq enrichment were clearly scored outside the *HoxC* cluster in the distal limb ectoderm, whereas they were not detected in the E13.5 forebrain ATAC-seq control dataset (Fig. 3*A*, third track). Furthermore, these two loci, as well as the *HoxC* cluster, were enriched in H3K4me2 in E10.5 ectoderm, a chromatin mark indicative of transcriptional and enhancer activity (Fig. 3*A*, *Bottom* track). The presence of other chromatin marks indicative of active enhancer regions using published limb bud datasets was not possible due to the high dilution of ectodermal cells in this material.

These two accessible regions, termed *EC1* and *EC2* (Enhancer of *HoxC* cluster 1 and 2), are located 165 and 81 kb upstream of the *HoxC* cluster, respectively, and are highly conserved among mammals in their DNA sequences, while absent from other vertebrate species (Fig. 3*B*). Based on this phylogenetic conservation, the *EC1* and *EC2* sequences were characterized as 1.1 and 4.1 kb large, respectively. Of note, the *EC1* sequence was conserved in placental mammals only, whereas *EC2* was conserved throughout mammals. We set up to assess the activity of these two sequences in transgenic mice either individually or in tandem, using an enhancer *LacZ* reporter construct. Transient transgenic fetuses were harvested at E16.5 and the activity of the reporter *LacZ* gene revealed in whole-mount β-gal staining (Fig. 3 *C–H*, Table 1, and see *SI Appendix*, Fig. S4). This time point was selected because at E16.5 the primitive nail matrix is already discernible as well as the primary and secondary HFs.

The *EC1* enhancer displayed a very strong, specific, and reproducible activity (five out of seven transgenic specimens) in the distal limb bud ectoderm and the developing tail. At the level of the mid zeugopod or the proximal tail, a dense pattern of staining progressively changed to mark HF exclusively. The HFs were stained over broad areas of the body, although transgene activity was not scored in the whisker pad (Fig. 3*C* and *SI Appendix*, Fig. S4). The *EC2* sequence elicited a similar activity, yet with a little more variability and smaller penetrance (7 out of 28 transgenic specimens). In general, the ectoderm area showing a dense staining was more restricted to the distal limb, and in most cases, staining was not detected in the tail. While variable areas of head ectoderm were also stained, the transgene did not seem to be active in whiskers, as for *EC1* (Fig. 3*D* and *SI Appendix*, Fig. S4).

In order to evaluate a potential collaborative or synergistic effect of *EC1* and *EC2*, we assayed their functional activity when introduced in tandem into the enhancer *LacZ* reporter construct. For this, *EC1* and *EC2* were fused one after the other with *EC2* positioned 5′ to *EC1*. In this combined situation, the *EC1–EC2*

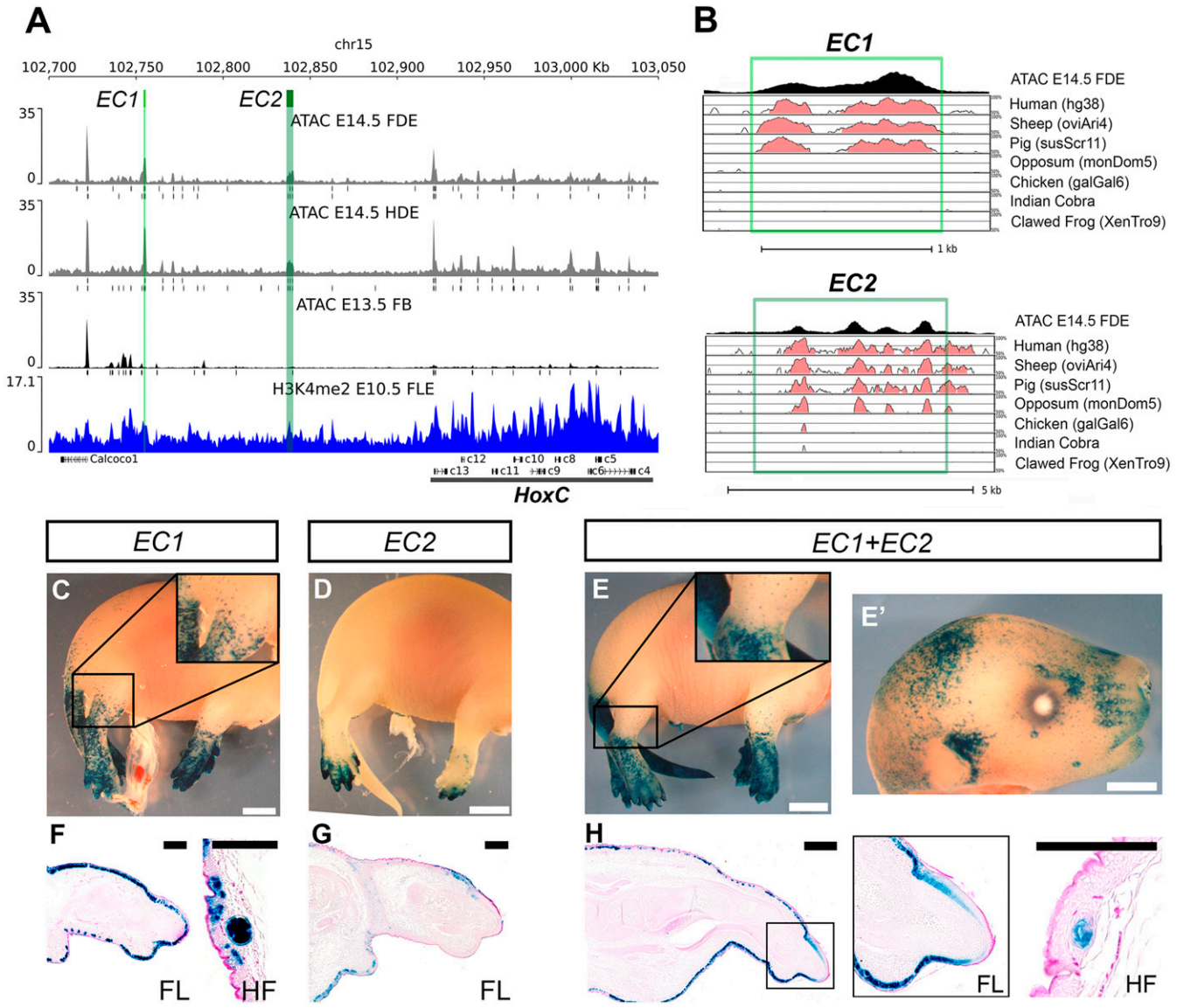

Fig. 3. Identification of ectodermal enhancers. (*A*) Coverage around the *HoxC* genomic locus of ATAC-seq signals obtained with E14.5 forelimb distal ectoderm (FDE) and hindlimb distal ectoderm (HDE) in gray (each one is the mean of two replicates) with the peak calling of each replicate as well as the ATAC-seq profile of E13.5 forebrain cells (FB) in black used as a negative control and H3K4me2 ChIP-seq in blue. The two peaks highlighted in green were identified by ATAC-seq only in the distal digit ectoderm but are absent from the control profile in forebrain cells. The ATAC-seq coverage were normalized by million reads in peaks. (*B*) Results of the mVISTA tool (shuffle-LAGAN) overlaid with the ATAC-seq coverage track of forelimb distal ectoderm (FDE) (top track). Conservation of *EC1* and *EC2* is assessed for seven different species. For each track, the identity over 100 bp is shown between 50% and 100%, and the pink color indicates over 70% of sequence identity. Note that *EC1* is conserved in placental mammals only (light green box), whereas *EC2* is conserved in all mammals (dark green box). The poor quality of the opossum genome around the *HoxC* cluster and the presence of gaps in both cobra and frog genomes must be kept in mind. (*C*–*E*′) Reporter activity of *EC1*, *EC2*, and *EC1+EC2* in E16.5 transgenic fetuses is shown by representative whole-mount *LacZ* expression patterns. Note the prominent *LacZ* staining in the tail and limb bud ectoderm. (Scale bars: 2 mm.) (*F*–*H*) Longitudinal sections of limb buds (dorsal up and distal to the right) showing expression restricted to the ectoderm. Magnifications of the hair follicles (HFs) in the proximal limb are also shown. (Scale bars: 150 μm.)

transgene displayed very robust and consistent reporter activity in the tail and distal limb ectoderm, as well as in HFs throughout the body surface (10 out of 14 transgenic specimens) (Fig. 3*E* and *SI Appendix*, Fig. S4). Reporter activity was also prominent in patches of head ectoderm, in the whisker pad, and eyelashes (Fig. 3*E*, Table 1, and *SI Appendix*, Fig. S4). Of note, the dorsal and ventral midlines and the genital tubercle were also stained (*SI Appendix*, Fig. S4).

Longitudinal sections of the limbs of stained embryos for each of the three transgenes confirmed the restriction of their activity to the ectodermal component and illustrated the transition from a distal stronger staining pattern, to a more proximal activity restricted to HFs (Fig. 3 *F*–*H*). Altogether, these results confirmed that both *EC1* and *EC2* control important aspects of *Hoxc* genes transcription in the ectoderm, both during early embryonic steps and during late phases of differentiation.

Deletions of *EC1* and *EC2* Enhancers in Mice. To further validate the functional contribution of these two potential enhancer sequences, we used CRISPR–Cas9 genome editing to generate mice lacking each of them, separately (Fig. 4*A*). Pairs of guide RNAs (gRNAs) were used to induce deletions covering either

Table 1. Summary of transgenic analyses

Transgene	Total no. of embryos analyzed*	No. (%) of transgenic embryos†	No. (%) of β-gal–stained embryos
EC1	23	7 (30.43%)	5 (71.43%)
EC2	112	28 (25%)	7 (25%)
EC1+EC2	39	14 (35.90%)	10 (71.43%)

*Embryos recovered from PNI.
†As determined by PCR on DNA from yolk sacs.

the *EC1* or the *EC2* sequences (*SI Appendix*, Table S3) and zygotes were transformed through electroporation. Stable lines were generated for both the $HoxC^{delEC1}$ and $HoxC^{delEC2}$ alleles and bred to homozygosity. Mice homozygous for each deletion were indistinguishable from their wild-type littermates in all gross aspects such as developmental growth, fertility, and viability. Likewise, no significant difference was detected in their ectodermal derivatives and their hair looked healthy and glossy, as well as the nails, which were apparently normal also in the histological analysis (Fig. 4 *B* and *C*). While more detailed

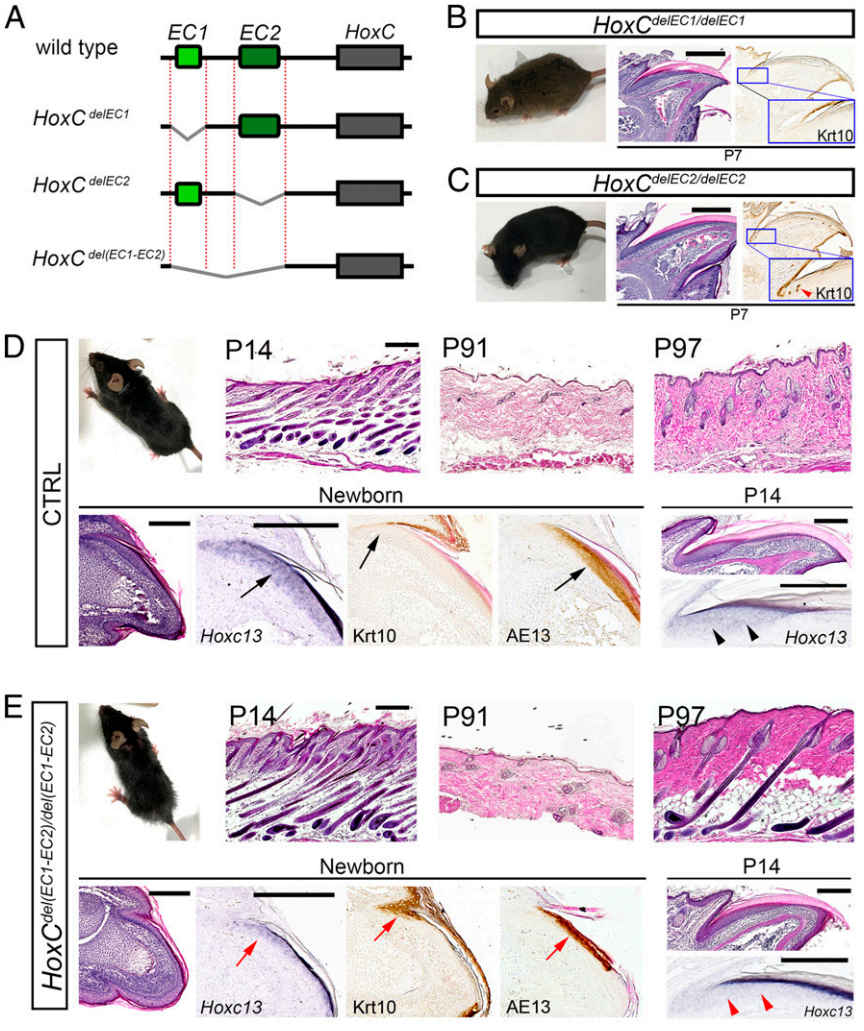

Fig. 4. Deletions of enhancers. (*A*) Schematic representation of the deletion alleles generated by CRISPR-Cas9. (*B*) $HoxC^{delEC1}$ homozygous mice were phenotypically like wild-type controls (*Left*) and showed normal nail development as can be observed in the hematoxylin–eosin (HE) longitudinal section (*Middle*) and anti-Krt10 staining (*Right*) ($n = 3$). (*C*) $HoxC^{delEC2}$ homozygous mice appeared normal as well (*Left*) and HE analysis did not show any alteration of the nail (*Middle*), although a minor ectopic expression of Krt10 was detected in the nail matrix (*Right*) (red arrowhead in magnified *Inset*) ($n = 3$). (Scale bars: *B* and *C*, 400 μm.) (*D* and *E*) Mice homozygous for the deletion of both enhancers ($HoxC^{del(EC1\text{-}EC2)/del(EC1\text{-}EC2)}$) displayed disheveled fur and hypoplastic nails. Histological comparison of HFs in HE-stained sections of dorsal skin from P14 control and $HoxC^{del(EC1\text{-}EC2)/del(EC1\text{-}EC2)}$ homozygous mice showed some hair shafts distorted at the level of the sebaceous glands (*E*). Over time, however, an acceleration in the cycling rate became evident as illustrated by mutant dorsal HFs having precociously entered the next anagen at P97, while control HFs remained in telogen as in P91 ($n = 2$). (Scale bars: *D* and *E*, 200 μm.) At birth, the mutant nails were hypoplastic as indicated by the abnormal expression of Krt10 remaining in the proximal nail matrix, and the substantial reduction in *Hoxc13* and hard keratins expression (red arrows in *E*), compared with wild-type control (black arrows in *D*) ($n = 2$). The nail defect was highly attenuated over the first 2 wk of postnatal development (P14) despite continued reduction in *Hoxc13* mRNA level (red arrowheads).

molecular analyses revealed a slightly abnormal ectopic expression of Krt10 in some cells of the nail matrix in $HoxC^{delEC2}$ homozygous mutants (Fig. 4*C*), the differentiation of the nail in $HoxC^{delEC1}$ homozygous mutants appeared completely normal (Fig. 4*B*). From these results, we concluded that neither *EC1* nor *EC2* was necessary for the transcription of *HoxC* cluster genes in the ectoderm, at least in the presence of the other enhancer sequence. This raised the possibility that the two sequences carried a redundant specificity and may thus compensate for one another, as was described for a number of related cases in distinct mammalian gene regulatory landscapes (35, 38, 39).

To investigate whether *EC1* and *EC2* may indeed share parts or all of their spatiotemporal regulatory specificities, we deleted a 86-kb-large DNA sequence containing the two sequences to produce the $HoxC^{del(EC1\text{-}EC2)}$ allele (Fig. 4*A*). Mice homozygous for this allele were viable and fertile. While they globally looked healthy, they exhibited mild but consistent fur and nail phenotypes (Fig. 4 *D* and *E*). When compared to control littermates, homozygous $HoxC^{del(EC1\text{-}EC2)}$ mice showed the persistence of a disheveled fur (a rough fur phenotype) with some of the mice developing bald patches on their backs. Histological analyses of the skin did not reveal any obvious defect in the morphogenesis of the HFs but showed some hair shafts distorted at the level of the sebaceous glands, reminiscent but less marked than those observed in *Hoxc13*-null and *Foxn1*-null mice and that associate with defective keratinization of the hair shaft (40). Over time, after the second or third hair cycles, an acceleration in the hair cycle became obvious. Therefore, when compared to wild-type littermates, homozygous $HoxC^{del(EC1\text{-}EC2)}$ mutants showed a precocious reinitiation of the next cycle with shortened telogen and premature anagen development, as shown in the analysis of postnatal day 91 (P91) and P97 littermates (Fig. 4 *D* and *E*). This is possibly driven by the loss of hair inducing a plucking effect similar to the situation described in *Foxn1*-null mice (41). The nails were unusually hypoplastic at birth, showing abnormal Krt10 expression in the proximal nail matrix as well as a substantial reduction in hard keratins expression (Fig. 4 *D* and *E*). Accordingly, $HoxC^{del(EC1\text{-}EC2)/del(EC1\text{-}EC2)}$ mutant specimens displayed a substantial reduction in *Hoxc13* level of mRNAs (Fig. 4 *D* and *E*). The nail defects became attenuated during the first 2 wk of postnatal life, and by P14, the histology of the nail was close to normal. These observations suggested that the presence of both *EC1* and *EC2* is required to reach a threshold in *Hoxc* genes mRNAs that is needed for the normal morphogenesis of epidermal organs. Alternatively, sequences other than *EC1* and *EC2* in the deleted 86-kb-large region may also contribute to the phenotype (see below).

To further document a possible role of *Hoxc* gene dosage in the development of ectodermal organs and to examine the function of *EC1* and *EC2* in this context, we looked at the phenotypic consequence of deleting the two *EC1* and *EC2* enhancers in a sensitized genetic background, where the expression of the presumptive target *Hoxc* genes was further reduced. We generated transheterozygous mice harboring either one of the single or combined enhancer deletions, over the full deletion of the entire *HoxC* cluster. Animals of the $HoxC^{del(EC1)/-}$ or $HoxC^{del(EC2)/-}$ genotypes showed no particular phenotype, indicating that the individual functional contribution of either the *EC1* or the *EC2* enhancers was dispensable even under conditions of sensitized background.

However, the removal of both enhancers on this same background ($HoxC^{del(EC1\text{-}EC2)/-}$) led to a striking phenotype characterized by the total absence of body hair (Fig. 5*A*). Transheterozygous $HoxC^{del(EC1\text{-}EC2)/-}$ mice were born at the expected Mendelian ratio and were viable and fertile. The phenotype became detectable shortly after birth due to their nude aspect (Fig. 5*A*). In contrast to heterozygous or wild-type control mice, no fur coat emerged from the skin of $HoxC^{del(EC1\text{-}EC2)/-}$ specimens during the first postnatal week, reminiscent of the phenotype of *Hoxc13* homozygous mutant animals (12). Interestingly, despite their lack of hairs, they displayed vibrissae at birth, in contrast to *Hoxc13* mutant mice. These mice remained nude until the new anagen phase, at about 5 wk of age, when they developed hairs in a cranio-caudal wave. The hairs were rapidly lost in the next couple of days, however, and the mice remained nude until the next hair cycle when a new wave of hairs emerged and was rapidly lost again. Thereafter, the waves of hair regrowth and loss became more irregular. This iterative pattern of hair formation and loss resulted in a typical cyclic alopecia phenotype (Fig. 5*A*).

At birth, the nails of $HoxC^{del(EC1\text{-}EC2)/-}$ mice were severely underdeveloped with only minor focal areas of specific nail

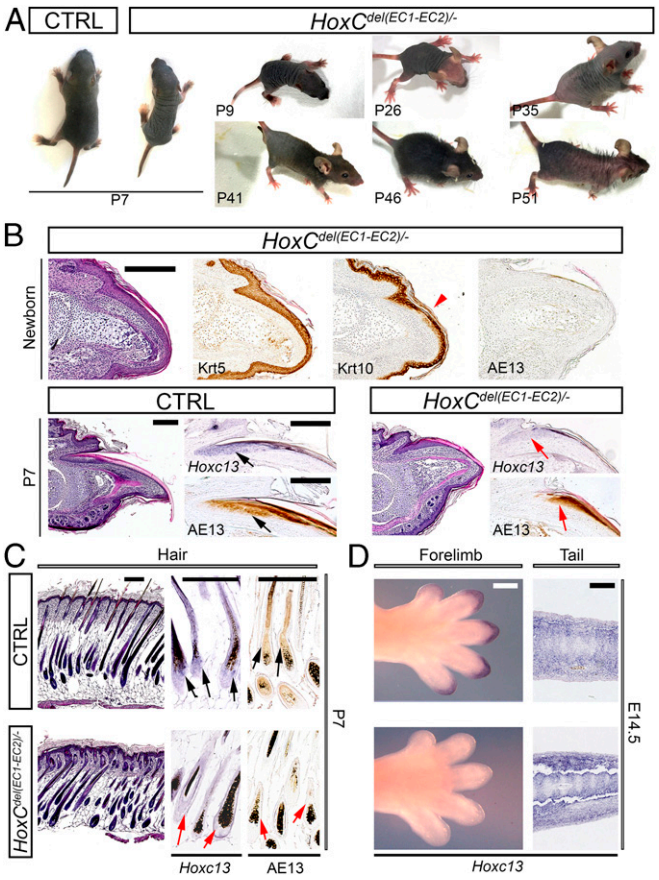

Fig. 5. Effects of *EC1* and *EC2* combined deletion in a sensitized background. (*A*) $HoxC^{del(EC1\text{-}EC2)/-}$ transheterozygous mice lack external hair during the first hair cycle and develop cyclic alopecia as can be observed in the displayed sequence ($n = 3$). (*B*) The characterization of $HoxC^{del(EC1\text{-}EC2)/-}$ nails revealed an underdeveloped organ at birth (top row), with only minor focal areas of specific nail differentiation marked by the down-regulation of Krt10 (arrowhead). Hard keratin expression was not scored (compare with Fig. 4*D*) ($n = 2$). The phenotype progressively attenuated with nail differentiation, as revealed by the expression of hard keratins (red arrow), observed in P7 mutant specimens, associated with a reduced level of *Hoxc13* mRNAs (red arrow) ($n = 2$). (Scale bars: 200 μm.) (*C*) Analysis of mutant $HoxC^{del(EC1\text{-}EC2)/-}$ HFs. On P7 dorsal skin, mutant mice showed a number of HFs that became distorted when entering the epidermis. This was accompanied by a down-regulation of *Hoxc13* expression (red arrows) and by a marked reduction of hard keratins detected by AE13 immunohistochemistry ($n = 2$). In *B* and *D*, the red arrows denote mutant altered expressions, while black arrows denote normal expression in controls. (*D*) At E14.5, *Hoxc13* expression was bellow detection level in the ectoderm of the digit tips of $HoxC^{del(EC1\text{-}EC2)/-}$ mutants, yet it persisted at a normal level in the tail mesenchyme ($n = 2$). (Scale bars: 400 μm.)

differentiation and a total absence of nail plate and hard keratin expression (Fig. 5*B*; compare with control in Figs. 2*D* and 4*D*), reminiscent of the $HoxC^{-/-}$ nail phenotype (Fig. 2). Over time (P7), however, the defect became less pronounced, although the expression of *Hoxc13* and hard keratins remained lower than normal. The nail and hair defects observed in $HoxC^{del(EC1\text{-}EC2)/-}$ mice were strikingly similar to that reported for mice lacking the *Foxn1* function, a gene known to be a transcriptional target of *Hoxc13* and, in turn, a transcriptional regulator of hard keratins of the hair shaft (40, 42). Accordingly, the histological analysis of HFs showed a phenotype similar to that described in *Foxn1*-null mice. HFs formed normally during fetal development but the hair shaft was distorted when entering the epidermis (Fig. 5*C*), a phenotype that was considered to derive from the lack of hard keratins in *Foxn1* mutants. Hard keratins were reduced substantially in the HFs of $HoxC^{del(EC1\text{-}EC2)/-}$ mice, correlating with a lower level of *Hoxc13* mRNAs.

The CRISPR-Cas9 approach also triggered an inversion of the targeted region producing the $HoxC^{inv(EC1\text{-}EC2)}$ allele. Mice homozygous for this allele ($HoxC^{inv(EC1\text{-}EC2/inv(EC1\text{-}EC2)}$) were indistinguishable from wild-type littermates and displayed normal fur and nails indicating that the inverted rearrangement of the enhancers had no functional consequence (*SI Appendix*, Fig. S5). In addition, mice transheterozygous for this inverted configuration and the deletion of the *HoxC* cluster ($HoxC^{inv(EC1\text{-}EC2)/-}$) did not show any abnormality (*SI Appendix*, Fig. S5).

These results suggested that both *EC1* and *EC2* contribute to the normal level of transcription of *Hoxc13* in the ectoderm. In contrast to both $Hoxc13^{-/-}$ (12, 13) and $HoxC^{-/-}$ (14) mutant mice, the hereby described $HoxC^{del(EC1\text{-}EC2)/-}$ mice were viable and healthy, indicating that the induced defects were likely localized to the reported ectodermal components. We further tested this hypothesis by looking at the expression of *Hoxc13* at E14.5, both in the limb ectoderm and in the growing tail mesenchyme, another site where *Hoxc13* is normally transcribed. While no detectable *Hoxc13* transcripts were scored in the limb ectoderm by whole-mount ISH, expression of this gene in the tail mesenchyme remained as in controls (Fig. 5*D*), supporting the definition of *EC1* and *EC2* as enhancers carrying a predominant ectodermal specificity.

To try to better quantify the functional impact of the *EC1* and *EC2* enhancers on the expression level of *Hoxc13*, we performed RT-qPCR using different mutant alleles (Fig. 6). We dissected out the distal aspects of E15.5 digits to isolate material corresponding to the region with the highest level of *Hoxc13* expression (Fig. 1*E*). $HoxC^{delEC1}$ homozygous showed a significant decrease of 40% in the steady-state level of *Hoxc13* mRNAs. A stronger decrease was observed for the $HoxC^{delEC2}$ homozygous samples, as only ~30% of the total amount of *Hoxc13* mRNAs were maintained, while $HoxC^{del(EC1\text{-}EC2)}$ homozygous samples displayed only 5% of the total amount of *Hoxc13* mRNAs. Other genetic combinations, such as the $HoxC^{del(EC1\text{-}EC2)/-}$ that displayed only 2% of *Hoxc13*, confirmed this range of effects (Fig. 6). Because neither $HoxC^{delEC1}$ nor $HoxC^{delEC2}$ homozygous embryos showed any clear phenotypic alteration, we conclude that the presence of 30% of the steady-state level of *Hoxc13* mRNAs is enough to ensure normal development of these ectodermal organs. Our results also reveal that a reduction in *Hoxc13* expression level from 5 to 2% of the wild-type level, determines the change from the disheveled phenotype of $HoxC^{del(EC1\text{-}EC2)/del(EC1\text{-}EC2)}$ to the cyclic alopecia of $HoxC^{del(EC1\text{-}EC2)/-}$ mutants. These results confirmed the functional importance of both enhancers, although with a more important contribution of *EC2*. Also, the respective effects of the two single enhancer deletions suggested that these two sequences may account for the global effect observed when deleting the large *EC1-EC2* DNA fragment. Accordingly, we consider it unlikely that other DNA sequences within this fragment have a strong involvement in regulating *Hoxc* genes during ectoderm development.

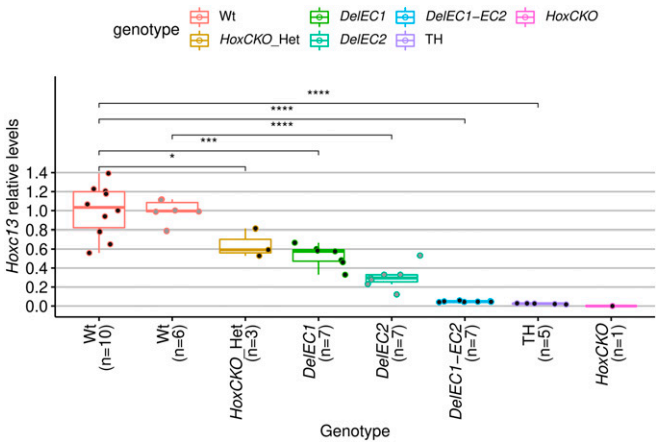

Fig. 6. Relative steady-state levels of *Hoxc13* mRNA in the various mutant alleles or combinations thereof. Comparative RT-qPCR analyses of *Hoxc13* mRNA levels in forelimb digit tips of E15.5 embryos of $HoxC^{delEC1/delEC1}$, $HoxC^{delEC2/delEC2}$, $HoxC^{del(EC1\text{-}EC2)/del(EC1\text{-}EC2)}$, $HoxC^{del(EC1\text{-}EC2)/-}$, $HoxC^{+/-}$, and $HoxC^{-/-}$, as indicated in the *x* axis. The *y* axis represents the level of expression of *Hoxc13* relative to control set to 1. The dissection in $HoxC^{delEC2/delEC2}$ samples included a larger digit segment than in the rest of genotypes, and therefore they were normalized by using similar dissections of control samples (gray dots). The addition of the negative effects observed independently in the single *EC1* and *EC2* deletion alleles approximately corresponds to the effect obtained by deleting the two enhancers at the same time. $*P \leq 0.05$; $***P \leq 0.001$; $****P \leq 0.0001$.

Discussion

We report here that the *HoxC* cluster has evolved a general functional specificity for some ectodermal organs, the nails and hairs, and that, at an earlier stage, *Hoxc* genes are activated in the embryonic limb ectoderm following a colinear time sequence. We also show that part of this subsequent specificity is achieved through the presence of two enhancers positioned at a distance from the gene cluster itself and acting together to raise the transcription level of a subgroup of *Hoxc* genes.

Colinear and Noncolinear Expression of *HoxC* Cluster Genes in the Ectoderm. During the formation and elongation of the major body axis, *Hox* genes belonging to all four gene clusters are activated in a time sequence that reflects their topological order along their respective clusters (32). While the impact of this temporal process upon the colinear distribution of *Hox* transcripts in space is still a matter of discussion (see, e.g., refs. 43–46), the mechanism underlying this phenomenon is accompanied by a progressive transition from a negative to a transcriptionally permissive chromatin structure (47). This phenomenon is however observed only during the first wave of activation of a given *Hox* cluster. Indeed, once the cluster open, global enhancers located in the surrounding regulatory landscapes can subsequently regulate subgroups of genes located *in cis* simultaneously, as was shown for example for the transcription of *Hoxd* genes in the developing digits or external genitals (48).

Here, we show a clear collinear time sequence in the activation of *Hoxc* genes in the limb ectodermal component. This temporal sequence in mRNAs production does not correspond to any distinct ectodermal structure or compartment, which could have required the proper deployment of various HOXC proteins in time and space, for example to identify different cell types produced through a developmental iteration. We interpret this as an indication that the *HoxC* cluster was initially not transcribed at

all in the ectodermal precursors and hence that its chromatin structure was not transcriptionally challenged before this precise spatiotemporal situation. As a consequence, upon activation, the gene cluster had to be processed like all *Hox* clusters during their initial phase of activation, following a 3′ (*Hoxc4* in this case) to 5′ (*Hoxc13*) direction. In this view, the temporal colinear activation we describe in the limb ectoderm may not reflect any particular functional constraint other than allowing eventually the transcription of the most 5′ located genes that seem to be required for the development of ectodermal organs. As such, it may illustrate an intrinsic constraint of the system (49). Alternatively, temporal colinearity in limb ectoderm may underlie the slightly different distributions of *Hoxc* genes, which in turn may impact the morphology of the nails.

In contrast, expression of *Hoxc* genes in HFs occurs throughout the body, with no particular rostral to caudal colinear distribution. For this reason, it was initially proposed to "break" spatial colinearity (12). In fact, this deviation from the spatial colinearity observed during the development of the major body axis is only detected in the ectodermal compartment, since *Hoxc* gene expression in the dermal papilla seems to be colinear indeed, with *Hoxc4* to *Hoxc10* transcribed in dorsal skin, whereas *Hoxc10* to *Hoxc13* mRNAs are found in the tail (19). Altogether, our results further document the functional co-option of at least *Hoxc13* (see below) for a late but critical function in the hair and nail epidermal organs. Of note, the two enhancers reported here are located outside of the *HoxC* cluster, a global regulatory strategy often associated to *Hox* loci and observed in many other developmental contexts (see refs. 37 and 50–52).

Subfunctionalization of *Hox* Clusters. All four *Hox* gene clusters in amniotes are involved in the specification of structures during the development of the major body axis, which is likely their most ancestral function. In addition to this function, conserved in most animals with a bilateral symmetry, clusters were subsequently co-opted for specific functions, after the rounds of genomic duplications (53, 54). For example, both the *HoxD* and *HoxA* clusters are necessary to properly develop limbs and external genitalia. Such cluster-specific functions may be redundant between gene clusters (as is the case in limbs and genitals), and hence the full assessment of such global specificities has been difficult to evaluate due to the experimental problems to produce multiple full *Hox* cluster deletions (8).

In the case of *HoxC*, however, its deletion alone induced a drastic phenotype associated with the ectodermal compartment, thus suggesting that no other *Hox* cluster is equally functional in these important organs, which could have compensated for the absence of *Hoxc* genes function. This is reenforced by the fact that only *Hoxc* genes were found clearly expressed in the developing limb ectoderm (Fig. 1*A*). This observation suggests that the functional co-option of the *HoxC* cluster into ectodermal organs occurred after the full set of genome duplications, potentially to take over the control of structural components of ectodermal tissue such as the hard keratins.

Without an extensive genetic analysis, it is difficult to determine how many *Hoxc* genes, and which ones, were involved in these two functional recruitments. Also, the situation may be slightly different for the nails and the HFs, indicating either distinct functional requirements for these two organs, or/and different modalities in the recruitment and implementation of enhancers. In the case of HFs, indeed, *Hoxc13* function seems to be sufficient as *Hoxc13*-null mice are nude (12, 13) and the analysis of these mutant mice revealed the function of this gene in the production of hard keratins and keratin-associated-proteins that are direct targets of *Hoxc13* (40, 55). In the absence of hard keratins, the hair shafts are brittle and readily break as they emerge through the skin surface, thus producing the nude phenotype. Likewise, the nails are fragile and twisted (12, 40). The *Foxn1* gene, whose null mutation generates a nude phenotype, was also described as a *Hoxc13* regulatory target during hair and nail differentiation (40, 42, 56).

In the case of the nail, the functional contribution of *Hoxc* genes seems to be slightly different from in the hair. Indeed, while nails of *Hoxc13* mutant mice are fragile (12, 13), we show here that their abnormal phenotype is more severe in the complete absence of the *HoxC* cluster. *HoxC*$^{-/-}$ mutant animals, which die as newborns due to defective lung development (14), show a congenital anonychia with no trace of nail-specific keratinocyte differentiation, a phenotype that thus far remained unnoticed. Therefore, other *Hoxc* genes, possibly *Hoxc12*, whose expression is similar to that of *Hoxc13* (18), could either have a function during nail development, or partially substitute for *Hoxc13* function when the latter is inactivated.

A Mammalian-Specific Up-Regulation? The critical importance of *Hoxc13* in mammalian hair and nail is also emphasized by the strikingly similar phenotypes resulting from loss-of-function conditions in different species including rabbits and pigs (33, 57, 58). In these cases, hair and nail differentiation is impaired in a way comparable to the murine situation. In addition, there are clear similarities with the human ECTD9 (OMIM 614931), also caused by the loss of function of *HOXC13*. ECTDs are a group of congenital disorders characterized by abnormal development of two or more ectodermal appendages, without other obvious systemic anomalies. Hairs are most commonly affected in association with alterations of the nails, teeth (anodontia or hypodontia), or sweat glands. Among the very rare ECTDs involving hair and nail exclusively is the ECTD9, which is caused by mutations in *HOXC13* (33, 59, 60).

While hairs are specific for mammals, different skin appendages exist in other vertebrates, which also express *Hox* genes during their development, like in feather buds (61). Terminal keratinized digit structures like nails also exist in all tetrapods, under a variety of forms, and, in the chick, expression of *Hoxc13* was observed in the tips of digits along with the development of claws (*SI Appendix*, Fig. S6). Therefore, it is likely that a sustained level of *Hoxc* genes is required throughout the tetrapods lineage, in conjunction with several ectodermal organs that involve high amounts of keratins, regardless of the final morphologies of these organs (hairs or feathers, nails or claws). Accordingly, *Hoxc* genes could be necessary to activate a "keratinization program," which would be interpreted differently depending on the phylogenetic context. The two global enhancer sequences we report in this study may be necessary for this ectodermal specific activation of *Hoxc* genes, as suggested by their behavior when introduced into transgenic mice and the phenotype resulting from their deletion.

This view is nevertheless difficult to reconcile with the fact that neither of these two ectodermal enhancers seems to be conserved outside mammals. For instance, it is not found in birds, neither at the syntenic position nor elsewhere, while one would expect the same ectodermal regulation to occur for this highly conserved gene cluster. In addition, the deletion of these two sequences led to a very severe decrease in *Hoxc13* mRNA levels, although with a phenotype weaker than that produced by the deletion of the gene cluster itself. One possible explanation to this paradox may rely upon the quantitative versus qualitative aspect of this regulation. The hypomorph phenotype observed in newborns when deleting the two enhancers may indeed reflect a basal level of regulation, independent from these two sequences, which could be sufficiently performant in nonmammalian species. In this view, it is conceivable that the requirement for HOXC proteins to accompany the development of ectodermal organs be slightly different in various classes of vertebrata, with a higher protein level necessary in mammals than in birds. It is thus possible that the *EC1* and *EC2* enhancers evolved along with the

mammalian lineage to progressively adjust the overall dose of HOXC proteins such as to achieve well-adapted ectodermal organs. In this scenario, these enhancers would thus be specific for mammals but involved in a function much more largely distributed within vertebrates.

At a more mechanistic level, it is difficult to distinguish between a simple additive effect of these two enhancers and a genuine synergistic effect. By using a single-cell ATAC-seq dataset recently generated from E11.5 mouse forelimb buds (62), we observed that most of the cells having these enhancers open were indeed ectodermal cells (*SI Appendix*, Fig. S7) and that all those cells but one showing ATAC-seq signals on both enhancers were ectodermal cells. These results thus confirm the conclusion that both *EC1* and *EC2* are specific ectodermal enhancers and indicate that the two sequences can function in the same cell. Further work will be necessary to investigate the nature of this collaborative regulation.

Materials and Methods

See extended methods provided in *SI Appendix*.

Mouse Strains and Animal Ethics. We have used the four $HoxC^{del(EC1)}$, $HoxC^{del(EC2)}$, $HoxC^{del(EC1\text{-}EC2)}$, and $HoxC^{inv(EC1\text{-}EC2)}$ mutant lines generated by CRISPR/Cas9 and the previously published $Hoxc13^{GFP}$ (63) and *HoxC* cluster deletion (14) strains. All animal procedures were conducted according to the European Union regulations and the 3R principles and were performed in agreement with the Swiss law on animal protection, under license no. GE 81/14 (to D.D.) and reviewed and approved by the Bioethics Committee of the University of Cantabria. All analyses were carried out on at least two independent specimens, and in many cases, three or more samples were analyzed.

Histological Analysis, Immunohistochemistry, and ISH. Dissected tissues were fixed in 4% paraformaldehyde and processed for paraffin embedding and microtomy. Hematoxylin–eosin staining, immunohistochemistry, and ISH were performed following standard procedures. The primary antibodies used were as follows: anti-Keratin 5 (Sigma; SAB4501651), anti-Keratin 10 (Biolegend; 905401), and anti-Pan-Cytokeratin (AE13; Santa Cruz; sc-57012).

RNA-Seq. For each of the 16 samples, RNA libraries were prepared using the Truseq Stranded mRNA Library Prep Library Preparation kit (Illumina; 20020594) and 100-bp single reads were generated.

ATAC-Seq and Mouse Transgenic Enhancer Assays. We performed ATAC-seq (64) on isolated ectodermal cells from the distal tips of wild-type E14.5 embryos. Two forelimb and two hindlimb biological replicates were generated, and each dataset was processed individually. ATAC-seq on E13.5 forebrain was used as control. The analysis of the conservation of the *EC1* and *EC2* enhancers was performed with mVISTA shuffle-LAGAN (65). The activity of *EC1*, *EC2*, and *EC1+EC2* was assayed in mouse transgenesis by using a vector carrying a β-globin minimal promoter and the *LacZ* coding sequence (pSK- LacZ). For the analysis of both enhancers, the *EC1* and *EC2* DNA fragments were cloned together, separated by a stretch of 41 random nucleotides, with *EC2* positioned 5′ to *EC1*.

CRISPR-Cas9 Modifications. The gRNAs used to generate the *delEC1*, *delEC2*, *del(EC1-EC2)*, and *inv(EC1-EC2)* mutant lines were designed with CHOPCHOP (https://chopchop.cbu.uib.no/). The gRNA sequences used in the CRISPR experiments are listed in *SI Appendix*, Table S3. The CRISPR-Cas9 methodology used to generate the *delEC1* and *delEC2* mouse alleles was adapted from Qin et al. (66) and the *del(EC1-EC2)* and *inv(EC1-EC2)* mouse alleles were generated with the Alt-R CRISPR-Cas9 System from IDT (https://eu.idtdna.com/pages/products/crispr-genome-editing/alt-r-crispr-cas9-system). The mutant lines were generated by electroporation.

B6CBAF1/J Fertilized eggs were collected from the oviducts of E0.5 pregnant females. The collected eggs cultured in WM medium were washed with Opti-MEM (Gibco; 31985-047) three times to remove the serum-containing medium. The eggs were then lined up in the electrode gap filled with the electroporation solution, electroporated, and transferred into pseudopregnant foster mice (66, 67).

RT-qPCR. Forelimb digits 2 to 5 (either the whole digit or the distal third phalanx region) from wild-type, $HoxC^{delEC1/delEC1}$, $HoxC^{delEC2/delEC2}$, $HoxC^{del(EC1\text{-}EC2)/del(EC1\text{-}EC2)}$, $HoxC^{+/-}$, and $HoxC^{-/-}$ embryos were dissected out in cold RNase-free PBS. Total RNA was extracted with RNeasy Plus Micro Kit (Qiagen) and 500 ng of total RNA was reverse transcribed to produce first-strand cDNA with iScriptTM cDNA Synthesis kit (Bio-Rad) using standard conditions. RT-qPCR was carried out on an Applied Biosystems StepOnePlus using NZYSpeedy qPCR Green Master Mix, ROX plus (NZYTech). The primers used to amplify *Hoxc13* were as follows: forward (Fwd), AGCACTGGGCTCTTTCCAAT (68), and reverse (Rev), CGGGCTGTAGAGGAACCACGT. PCR efficiencies were measured using serial dilutions of cDNA. Relative transcript levels were normalized to GAPDH (Fwd, TGCAGTGGCAAAGTGGAGAT; Rev, ACTGTGCCG TTGAATTTGCC). Between 5 and 10 biological replicates were analyzed for each genotype, with 3 technical replicates for each sample. The expression levels of mutant samples were calculated relative to wild-type controls (average set to 1). Significance of differences were determined using the two-tailed, Welsh *t* test.

Data Availability. All raw and processed datasets of RNA-seq and ATAC-seq have been deposited in the Gene Expression Omnibus (GEO) repository (accession no. GSE150702). All sequences used for conservation analysis as well as all bioinformatics scripts needed to reproduce the figures from raw data have been deposited at GitHub, https://github.com/lldelisle/scriptsForFernandezGuerreroEtAl2020. The raw and process datasets of the H3K4me2 ChIP-seq are registered under GSM4294458 (https://doi.org/10.1101/2020.02.26.965178).

ACKNOWLEDGMENTS. We thank Sara Lucas, Bea Romero, Mar Rodriguez, and Bénédicte Mascrez for their help with electroporation of embryos and handling crosses as well as Laura Galán for excellent technical assistance. This work was supported by funds from the Ecole Polytechnique Fédérale (Lausanne), the University of Geneva and the Swiss National Research Fund (310030B_138662), and the European Research Council grants Regul*Hox* (588029) to D.D., and by the Spanish Ministry of Science and Innovation (Grant BFU2017-88265-P) to M.A.R.

1. J. Zakany, D. Duboule, The role of Hox genes during vertebrate limb development. *Curr. Opin. Genet. Dev.* **17**, 359–366 (2007).
2. J. M. Woltering, D. Noordermeer, M. Leleu, D. Duboule, Conservation and divergence of regulatory strategies at hox loci and the origin of tetrapod digits. *PLoS Biol.* **12**, e1001773 (2014).
3. M. Kmita *et al.*, Early developmental arrest of mammalian limbs lacking HoxA/HoxD gene function. *Nature* **435**, 1113–1116 (2005).
4. A. M. Boulet, M. R. Capecchi, Multiple roles of Hoxa11 and Hoxd11 in the formation of the mammalian forelimb zeugopod. *Development* **131**, 299–309 (2004).
5. A. P. Davis, D. P. Witte, M. H.-L. Hsiu, S. S. Potter, M. R. Capecchi, Absence of radius and ulna in mice lacking hoxa-11 and hoxd-11. *Nature* **375**, 791–795 (1995).
6. D. M. Wellik, M. R. Capecchi, Hox10 and Hox11 genes are required to globally pattern the mammalian skeleton. *Science* **301**, 363–368 (2003).
7. B. Xu, D. M. Wellik, Axial Hox9 activity establishes the posterior field in the developing forelimb. *Proc. Natl. Acad. Sci. U.S.A.* **108**, 4888–4891 (2011).
8. N. Soshnikova, R. Dewaele, P. Janvier, R. Krumlauf, D. Duboule, Duplications of *hox* gene clusters and the emergence of vertebrates. *Dev. Biol.* **378**, 194–199 (2013).
9. V. J. Lynch *et al.*, Adaptive evolution of HoxA-11 and HoxA-13 at the origin of the uterus in mammals. *Proc. Biol. Sci.* **271**, 2201–2207 (2004).
10. V. J. Lynch *et al.*, Adaptive changes in the transcription factor HoxA-11 are essential for the evolution of pregnancy in mammals. *Proc. Natl. Acad. Sci. U.S.A.* **105**, 14928–14933 (2008).
11. V. J. Lynch, K. Brayer, B. Gellersen, G. P. Wagner, HoxA-11 and FOXO1A cooperate to regulate decidual prolactin expression: Towards inferring the core transcriptional regulators of decidual genes. *PLoS One* **4**, e6845 (2009).
12. A. R. Godwin, M. R. Capecchi, Hoxc13 mutant mice lack external hair. *Genes Dev.* **12**, 11–20 (1998).
13. A. R. Godwin, M. R. Capecchi, Hair defects in Hoxc13 mutant mice. *J. Investig. Dermatol. Symp. Proc.* **4**, 244–247 (1999).
14. H. Suemori, S. Noguchi, Hox C cluster genes are dispensable for overall body plan of mouse embryonic development. *Dev. Biol.* **220**, 333–342 (2000).
15. A. Awgulewitsch, Hox in hair growth and development. *Naturwissenschaften* **90**, 193–211 (2003).
16. A. I. Reid, S. J. Gaunt, Colinearity and non-colinearity in the expression of Hox genes in developing chick skin. *Int. J. Dev. Biol.* **46**, 209–215 (2002).
17. B. Kanzler, J. P. Viallet, H. Le Mouellic, D. Duboule, D. Dhouailly, Differential expression of two different homeobox gene families during mouse tegument morphogenesis. *Int. J. Dev. Biol.* **38**, 633–640 (1994).
18. L. Shang, N. D. Pruett, A. Awgulewitsch, Hoxc12 expression pattern in developing and cycling murine hair follicles. *Mech. Dev.* **113**, 207–210 (2002).
19. Z. Yu *et al.*, Hoxc-dependent mesenchymal niche heterogeneity drives regional hair follicle regeneration. *Cell Stem Cell* **23**, 487–500 (2018).
20. J. M. Cairns, J. W. Saunders, The influence of embryonic mesoderm on the regional specification of epidermal derivatives in the chick. *J. Exp. Zool.* **127**, 221–248 (1954).

21. L. C. Biggs, M. L. Mikkola, Early inductive events in ectodermal appendage morphogenesis. *Semin. Cell Dev. Biol.* **25–26**, 11–21 (2014).
22. M. Saito, M. Ohyama, M. Amagai, Exploring the biology of the nail: An intriguing but less-investigated skin appendage. *J. Dermatol. Sci.* **79**, 187–193 (2015).
23. C. P. Lu, L. Polak, B. E. Keyes, E. Fuchs, Spatiotemporal antagonism in mesenchymal-epithelial signaling in sweat versus hair fate decision. *Science* **354**, aah6102 (2016).
24. D. Summerbell, J. H. Lewis, L. Wolpert, Positional information in chick limb morphogenesis. *Nature* **244**, 492–496 (1973).
25. N. Vargesson *et al*., Cell fate in the chick limb bud and relationship to gene expression. *Development* **124**, 1909–1918 (1997).
26. K. Sato, Y. Koizumi, M. Takahashi, A. Kuroiwa, K. Tamura, Specification of cell fate along the proximal-distal axis in the developing chick limb bud. *Development* **134**, 1397–1406 (2007).
27. D. L. Chapman *et al*., Expression of the T-box family genes, Tbx1-Tbx5, during early mouse development. *Dev. Dyn.* **206**, 379–390 (1996).
28. M. Fernandez-Teran, M. A. Ros, The apical ectodermal ridge: Morphological aspects and signaling pathways. *Int. J. Dev. Biol.* **52**, 857–871 (2008).
29. R. A. Ihrie *et al*., Perp is a p63-regulated gene essential for epithelial integrity. *Cell* **120**, 843–856 (2005).
30. S. Kuratani *et al*., The expression pattern of the chick homeobox gene gMHox suggests a role in patterning of the limbs and face and in compartmentalization of somites. *Dev. Biol.* **161**, 357–369 (1994).
31. P. Lertkiatmongkol, D. Liao, H. Mei, Y. Hu, P. J. Newman, Endothelial functions of platelet/endothelial cell adhesion molecule-1 (CD31). *Curr. Opin. Hematol.* **23**, 253–259 (2016).
32. M. Kmita, D. Duboule, Organizing axes in time and space; 25 years of collinear thinkering. *Science* **301**, 331–333 (2003).
33. Z. Lin *et al*., Loss-of-function mutations in HOXC13 cause pure hair and nail ectodermal dysplasia. *Am. J. Hum. Genet.* **91**, 906–911 (2012).
34. J. F. Peterson, J. Hartman, L. Ghaloul-Gonzalez, U. Surti, J. Hu, Absence of skeletal anomalies in siblings with a maternally inherited 12q13.13-q13.2 microdeletion partially involving the HOXC gene cluster. *Am. J. Med. Genet. A.* **164**, 810–814 (2014).
35. T. Montavon *et al*., A regulatory archipelago controls hox genes transcription in digits. *Cell* **147**, 1132–1145 (2011).
36. S. Delpretti *et al*., Multiple enhancers regulate hoxd genes and the hotdog LncRNA during cecum budding. *Cell Rep.* **5**, 137–150 (2013).
37. S. Berlivet, D. Paquette, D. Langlais, J. Dostie, M. Kmita, Clustering of tissue-specific sub-TADs accompanies the regulation of HoxA genes in developing limbs. *PLoS Genet.* **9**, 1–17 (2013).
38. N. Frankel *et al*., Phenotypic robustness conferred by apparently redundant transcriptional enhancers. *Nature* **466**, 490–493 (2010).
39. M. Osterwalder *et al*., Enhancer redundancy provides phenotypic robustness in mammalian development. *Nature* **554**, 239–243 (2018).
40. C. S. Potter *et al*., The nude mutant gene Foxn1 is a HOXC13 regulatory target during hair follicle and nail differentiation. *J. Invest. Dermatol.* **131**, 828–837 (2011).
41. N. Suzuki, M. Hirata, S. Kondo, Traveling stripes on the skin of a mutant mouse. *Proc. Natl. Acad. Sci. U.S.A.* **100**, 9680–9685 (2003).
42. L. Mecklenburg *et al*., FOXN1 is critical for onycholemmal terminal differentiation in nude (Foxn1nu) mice. *J. Invest. Dermatol.* **123**, 1001–1011 (2004).
43. J. Deschamps, D. Duboule, Embryonic timing, axial stem cells, chromatin dynamics, and the Hox clock. *Genes Dev.* **31**, 1406–1416 (2017).
44. A. J. Durston, Some questions and answers about the role of hox temporal collinearity in vertebrate axial patterning. *Front. Cell Dev. Biol.* **7**, 257 (2019).
45. T. Iimura, O. Pourquié, Hox genes in time and space during vertebrate body formation. *Dev. Growth Differ.* **49**, 265–275 (2007).
46. P. Tschopp, B. Tarchini, F. Spitz, J. Zakany, D. Duboule, Uncoupling time and space in the collinear regulation of Hox genes. *PLoS Genet.* **5**, e1000398 (2009).
47. N. Soshnikova, D. Duboule, Epigenetic temporal control of mouse hox genes in vivo. *Science* **1187**, 1320–1323 (2009).
48. T. Montavon, J. F. Le Garrec, M. Kerszberg, D. Duboule, Modeling Hox gene regulation in digits: Reverse collinearity and the molecular origin of thumbness. *Genes Dev.* **22**, 346–359 (2008).
49. D. Duboule, The rise and fall of Hox gene clusters. *Development* **134**, 2549–2560 (2007).
50. G. Andrey *et al*., A switch between topological domains underlies HoxD genes collinearity in mouse limbs. *Science* **340**, 1234167 (2013).
51. R. Schep *et al*., Control of Hoxd gene transcription in the mammary bud by hijacking a preexisting regulatory landscape. *Proc. Natl. Acad. Sci. U.S.A.* **113**, E7720–E7729 (2016).
52. F. Spitz, F. Gonzalez, D. Duboule, A chromosomal regulatory landscape containing the HoxD cluster franc. *Cell* **113**, 405–417 (2003).
53. S. Ohno, *Evolution by Gene Duplication* (Springer, Berlin, 1970).
54. P. W. H. Holland, Evolution of homeobox genes. *Wiley Interdiscip. Rev. Dev. Biol.* **2**, 31–45 (2013).
55. L. F. Jave-Suarez, H. Winter, L. Langbein, M. A. Rogers, J. Schweizer, HOXC13 is involved in the regulation of human hair keratin gene expression. *J. Biol. Chem.* **277**, 3718–3726 (2002).
56. S. P. Flannagan, "Nude," a new hairless gene with pleiotropic effects in the mouse. *Genet. Res.* **8**, 295–309 (1966).
57. J. Deng *et al*., The disrupted balance between hair follicles and sebaceous glands in Hoxc13-ablated rabbits. *FASEB J.* **33**, 1226–1234 (2019).
58. K. Han *et al*., Generation of Hoxc13 knockout pigs recapitulates human ectodermal dysplasia–9. *Hum. Mol. Genet.* **26**, 184–191 (2017).
59. M. Farooq *et al*., A homozygous frameshift mutation in the HOXC13 gene underlies pure hair and nail ectodermal dysplasia in a Syrian family. *Hum. Mutat.* **34**, 578–581 (2013).
60. A. K. Khan *et al*., A novel mutation in homeobox DNA binding domain of HOXC13 gene underlies pure hair and nail ectodermal dysplasia (ECTD9) in a Pakistani family. *BMC Med. Genet.* **18**, 1–5 (2017).
61. C. M. Chuong *et al*., Gradients of homeoproteins in developing feather buds. *Development* **110**, 1021–1030 (1990).
62. I. Desanlis *et al*., HOX13-dependent chromatin accessibility modulates the target repertoires of the HOX factors. https://doi.org/10.1101/789875 (25 May 2020).
63. A. R. Godwin, H. S. Stadler, K. Nakamura, M. R. Capecchi, Detection of targeted GFP-Hox gene fusions during mouse embryogenesis. *Proc. Natl. Acad. Sci. U.S.A.* **95**, 13042–13047 (1998).
64. J. Buenrostro, B. Wu, H. Chang, W. Greenleaf, ATAC-seq: A method for assaying chromatin accessibility genome-wide. *Curr. Protoc. Mol. Biol.* **109**, 1–21 (2016).
65. K. A. Frazer, L. Pachter, A. Poliakov, E. M. Rubin, I. Dubchak, VISTA: Computational tools for comparative genomics. *Nucleic Acids Res.* **32**, 273–279 (2004).
66. W. Qin *et al*., Efficient CRISPR/Cas9-Mediated genome editing in mice by zygote electroporation of nuclease. *Genetics* **200**, 423–430 (2015).
67. M. Hashimoto, T. Takemoto, Electroporation enables the efficient mRNA delivery into the mouse zygotes and facilitates CRISPR/Cas9-based genome editing. *Sci. Rep.* **5**, 11315 (2015).
68. R. Aires *et al*., Tail bud progenitor activity relies on a network comprising Gdf11, Lin28, and Hox13 genes. *Dev. Cell* **48**, 383–395.e8 (2019).